J Mater Sci (2010) 45:2625–2632
DOI 10.1007/s10853-010-4240-y

Chemically modified fly ash for fabricating super-strong biodegradable poly(vinyl alcohol) composite films

Dilip Chandra Deb Nath · Sri Bandyopadhyay · Philip Boughton · Aibing Yu · Darryl Blackburn · Chris White

Received: 5 December 2009 / Accepted: 13 January 2010 / Published online: 29 January 2010

Abstract Composite films of poly(vinyl alcohol) (PVA) and chemically modified fly ash (MFA) by sodium hydroxide were prepared by aqueous cast method with 5, 10, 15, 20 and 25 wt% MFA treated with 1 wt% cross-linking agent (glutaraldehyde, GLA). The tensile strengths of the composite films were found to increase proportionally with MFA and the maximum strength attained was 414% higher in the case of 20 wt% MFA than that in neat PVA film. The percentage of strain at break exponentially decreased with addition of MFA. The modulus of the composites was determined to increase proportionally up to a maximum 685% at 20 wt% MFA compared to that of neat PVA film. Interfacial networking between the MFA and PVA was evident from scanning electron microscopy (SEM) images of tensile-fractured surfaces, which was not observed for the unmodified fly ash (FA) system. Atomic force microscopy (AFM) analysis showed that the mean square surface roughness of the composite films of PVA–MFA was 53% smoother than the films with FA.

Introduction

Composite materials of polymers and inorganic fillers can result in higher modulus, strength, heat resistance, and low the gas permeability and flammability compared to neat polymers and fillers [1]. The mechanical properties of composites generally depend on the filler's nature, size and distribution, aspect ratio, volume fraction, and the intrinsic adhesion between the surfaces of filler and polymer [2]. High aspect ratio (fibre type) fillers generally increase the yield strength because the filler is capable of attaining high local stress transfer from the polymer matrix [3].

The development of stronger interfacial bonds within composites can result in increased rigidity. In order to provide stronger interfacial interaction between filler and polymer, functional group-based polymers may be selected. PVA is one of the biodegradable and water-soluble biopolymer candidates used in the fabrication of environmentally compatible composites. Fillers utilized in PVA composites include: sugar cane [4], starch [5], clay [6], carbon nanotube [7], wood dust [8], cement [9], organo-ceramic [10] and TiO_2 [11]. PVA and its composites have found wide use in a variety of industrial applications. Some of these uses include: fibre and textiles industries for sizing and finishing, coating, adhesives, emulsifiers, colloidal stabilizers and film packaging in food and optical holographic industries [12].

FA powder makes up a major proportion of industrial by-product. It is generated in thermal power stations during coal burning for the generation of electricity. The storage and handling of FA are challenges that need to be addressed from a sustainable development and environmental conservation angle. FA is commonly disposed of in dams and lagoons as landfill. This is not ideal as FA consists of mixtures of alkali and transition metal oxides, mainly of silicon, aluminium and iron, and small percentage of calcium, magnesium, potassium, sodium and titanium depending on the quality of coal and processing condition [13, 14]. Research into recycling and reuse of FA as filler in green and eco-friendly composite products is under way. It is being considered for use in composites

D. C. D. Nath · S. Bandyopadhyay (✉) · P. Boughton · A. Yu
School of Material Science and Engineering, The University of New South Wales, Kensington, NSW, Australia
e-mail: S.Bandyopadhyay@unsw.edu.au

D. Blackburn · C. White
Research and Ash Development, Cement Australia, Brisbane, QLD, Australia

with metal [15] and polymers. Polymers being filled with FA include polyester [16], epoxy [17], polypropylene (PP) [18–20] and PVA [21–23].

The tensile strength of PP and FA composite materials dramatically decrease with the addition of spherical particles FA at room temperature test [18]. In a previous study by the authors, improvements in mechanical strength were observed for FA-reinforced PVA composite films compared to neat PVA with 20% FA addition [21]. Chemical modification of FA particles is a possible method to obtain further increase in composite mechanical strength. The activation reactions of FA with alkali, sodium and potassium hydroxides, sodium silicate and sodium aluminate have been reported in the formation of cement pastes [24–29]. The activated-FA particles significantly enhance the setting properties and mechanical performance of cement [24].

The activation reaction is mediated by the breaking of covalent bonds, Si–O–Si and Al–O–Al in FA components then resulting in the formation of aluminate silicate [27]. The newly crystallized structures are the mixtures of zeolite family, e.g. faujasite, phillipsite and hydroxysodalite [28, 29]. The –OH concentration, curing time and temperature, type of alkaline media and bulk matter of FA are all critical factors in the control of mechanical strength of the cementitious materials [27].

Taking into consideration of the alkaline activation process of FA particles, the objective of this study is to determine whether further enhancements in mechanical strength of the PVA composite films can be achieved using MFA.

Experimental section

Materials

FA sample was obtained from Swanbank Coal Fire Plant, Cement Australia, Qld. Poly(vinly alcohol) (PVA) (Mw: 125,000 and degree of hydrolysis approx. 89%) from Fine-Chemical Ltd., Glutaraldehyde (GLA) (25% contents in water) from Laboratory Unilab Reagent, and reagent grade sodium hydroxide (NaOH) pellets were purchased and used as received.

Preparation of MFA by NaOH

First, 2 M NaOH solution was prepared using deionised water. After cooling the solution, 100 mL was delivered into a two-necked round bottom flask with attached condenser. This was placed in oil bath and actuated with a magnetic stirrer. Then, 15 g of FA particles was added and in and the mixture was sealed. The suspension was heated under vigorous stirring at 85 °C for 8 h. The cooled suspension was filtered and washed several times with deionised water. Finally the MFA was dried under vacuum for 2 days at 50 °C [22–30]. Compared to the 2 M NaOH selected in this study, the higher concentrations of NaOH (8–12 M at pH $>$ 12) and fly ash/NaOH = 1/1.2 were also reported for activation of fly ash [30, 31].

Preparation of PVA–MFA composite films

The composite films were fabricated by casting from aqueous mixtures of PVA and MFA. The neat PVA was dissolved in distilled water at 80 °C to prepare the 1.2% solution. The MFA particles with 5, 10, 15, 20 and 25 wt% concentrations were dispersed and sonicated for 5 min (Ultrasonic cleaner, FXPQM, frequency, 50 MHz). For the preparation of cross-linked composite films, 1 N HCl (50 μmL) and 1 wt% GLA aqueous solutions (0.50 mL) were added sequentially to PVA–MFA mixtures. The resulting mixtures were cast in glass petri-dishes. Bubbles were removed by shaking and blowing air. The cast petri-dishes were kept at room temperature until dried. The films were peeled out and dried in oven at 60 °C under vacuum for 6 h. The thickness of the films was 0.05–0.07 mm. The thickness of the films was controlled by using the same amount of total materials (400 mg for single casting) and same sized glass petri-dish (10 cm diameter) [7, 8, 21–23].

Testing methods

Tensile testing

The mechanical properties such as tensile yield strength, strain to break and modulus of elasticity were determined from tensile tests using an Instron 1185 with crosshead movement 50 mm/min. The specimens were prepared according to ASTM D882-95a (length 22 mm, width 5 mm and thickness 0.05 mm) [6, 8, 21–23]. Five samples were tested in each category and to then provide average values.

Scanning electron microscope (SEM)

A Hitachi 4500-II scanning electron microscope was used to examine the morphology of tensile-fractured surface composite films. The electrically non-conductive surfaces of FA and composites were coated in a chromium sputter unit by chromium. The two coating cycles were chosen to improve the conductivity of film surface for better images.

Atomic force microscopy (AFM)

The surface topography of the composites was investigated by AFM, Digital Instrument 3000 AFM in contact mode.

Cantilevers in contact mode probes were installed with low spring constants (<1 N/m) to minimize the force between the tip and the sample surface during imaging. Digital Silicon Nitride Probes (DNP) with 0.58 N/m cantilever were used for the AFM. DNP probe specifications (as supplied): Force (or Spring) constants 0.58, 0.32, 0.12, 0.06 N/m, Nominal tip radius of curvature > 10 nm, Cantilever lengths 100 and 200 μm, Tip height 2.5–3.5 μm, Cantilever configuration triangular, Reflective coating gold, Tip angles 35° on each side, 35° front, 35° back.

Infrared spectroscopy (FTIR)

Composites were characterized by FTIR spectroscope (NEXUS-870, Thermo Nicolet Corporation) running with Omnic software. The condition for the measurement of FTIR: detector, MCT/A; base splitter, KBr; window, diamond; velocity, 0.6329; aperture, 100; scan, 64.

Results and discussion

Morphological features of MFA

The characteristic studies of FA and MFA particles in the concept of particle size distributions, chemical and mineralogical compositions were reported recently along with an approach for potential application [22]. The major percentage mullite of FA is not an in ingredient of the sources of FA coal. The formation of mullite is occurred in the process of thermal decomposition of natural mineral kaolinite in coal combustion process [9], whereas the chemical reactions and thermodynamic studies of activation fly ash with sodium hydroxide were revealed the formation of new crystalline phase zeolite [25, 26].

Figure 1a and b shows TEM images of fly ash particles to illustrate the morphological changes by chemical activation. The existences of interfacial interactions amongst ash particles are distinctively clear with visible clouds in Fig. 1a. This particle–particle interfacial interaction completely disappeared along with narrower crystalline needle-like shape which will have higher aspect ratio as seen in MFA particles in Fig. 1b.

The spherical particles generally led to decrease in the mechanical strength of the composites. The decreasing in mechanical strength is thought to be derived from the weak or absence of interfacial interactions between the polymer and filler due to lower aspect ratio of spherical particles [18]. The couple of phenomena of MFA would contribute to better interfacial interaction of polymer matrix and fly ash filler and would have critical impact on mechanical strength of composite films as higher level of interfacial

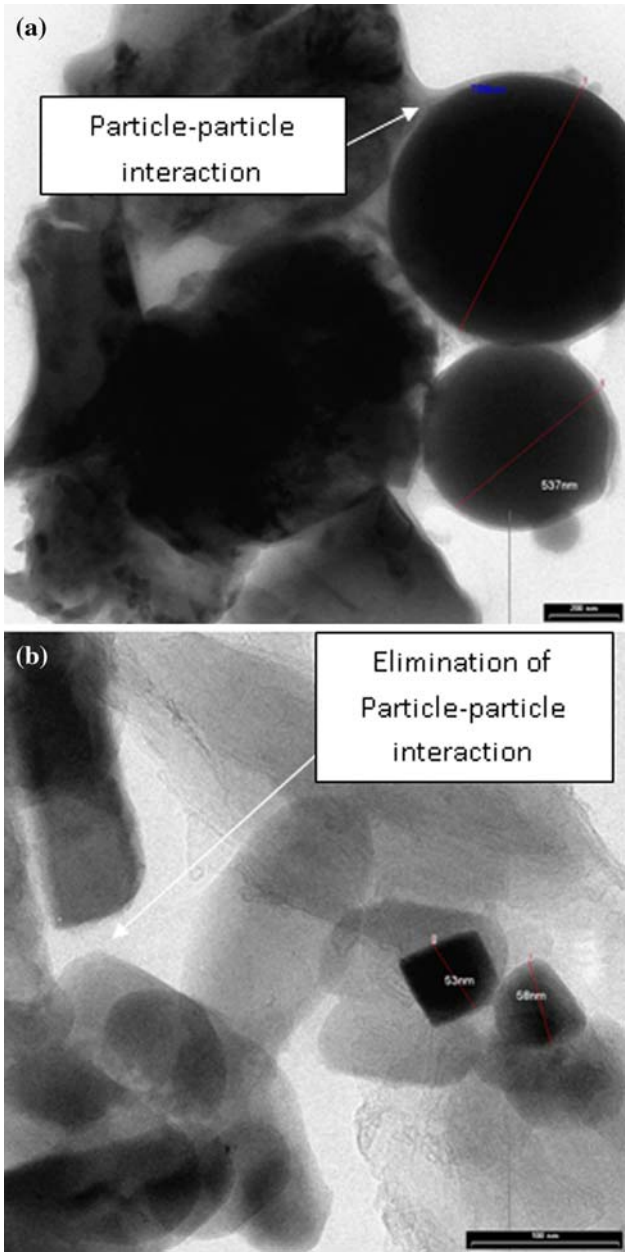

Fig. 1 TEM morphology images of fly ashes, **a** FA (spherical particles with particle–particle interaction) and **b** MFA (needle-like shape with no particle–particle interaction)

interaction leads to higher mechanical strength of composite materials by addressing physical/chemical bonding [4, 21].

Mechanical properties of neat PVA and composite films

The calculated tensile strength, strain at break and modulus from the stress–strain relationship diagrams of neat PVA and composites with 5, 10, 15, 20 and 25 wt% of MFA along with 1 wt% GLA are presented in Table 1.

Table 1 Mechanical properties of PVA–MFA composite films

MFA (wt%)	Cross-linking agent (wt%)	Tensile strength (MPa)	Strain at break (%)	Modulus (MPa)
0	–	28.2 ± 0.9	238 ± 10	120
20 (FA)	1	37.1 ± 2	87 ± 5	123
5	1	40.2 ± 2	26 ± 4	422
10	1	73.6 ± 3	56 ± 3	451
15	1	129.8 ± 3	68 ± 5	773
20	1	144.2 ± 2	37 ± 5	942
25	1	35.5 ± 4	26 ± 4	335

The addition of MFA to neat PVA proportionally improved the tensile strength, up to 20 wt% MFA concentration. A further addition of 25 wt% led to significant decrease. The decrease is assumed from the super-saturation of particles in composite films which led the enhancement of particle–particle interfacial interaction rather than particle–PVA interaction. The strain at break shows the reverse order of tensile strength with addition of MFA, indicating the existence of stronger interfacial interactions in the ternary systems, PVA, MFA and GLA. PVA is a matrix that readily facilitates the formation of intra and inter molecular hydrogen bonding between the –OH and $–COOCH_3$ groups present in the backbone of PVA chain [12]. The –OH groups present on the surface of fly ash particle take part in the formation of physical bonding between the PVA and FA [21], and chemically cross-linked with GLA molecules.

The insolubilization of PVA by cross-linking, acetalization reactions of intra and inter molecular chains have also been reported with acid-catalysed glyoxal, glutaraldehyde and terephthalaldehyde [32]. The formation of interfacial interactions play a significant role in improvement of mechanical strength compared to neat PVA, whereas the tensile strength in the composite of PP are reduced with addition of FA at room temperature investigation [18]. The non-polar PP has less chance to form a physical and/or chemical interfacial interaction zone with the FA surface.

The effect of modification of FA on mechanical properties

The effect of FA modifications in PVA–MFA composite films were investigated in the mechanical terms. The results were compared to those of the composite films with FA. The tensile strengths, strain at break and modulus (Young modulus) of the composite films were plotted as a function of MFA/FA under similar conditions in Figs. 2, 3 and 4, respectively.

The composite films with MFA showed higher tensile strengths than those of films with FA. The increase was up

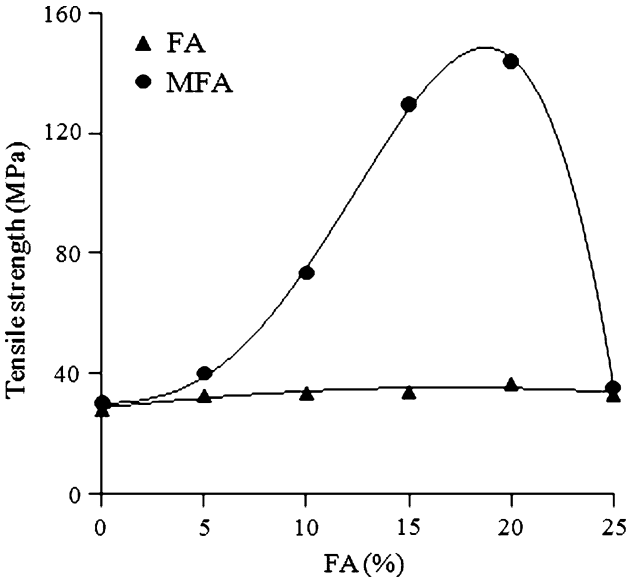

Fig. 2 Effect of chemical modification on the relationship of tensile stress and fly ash in composite films

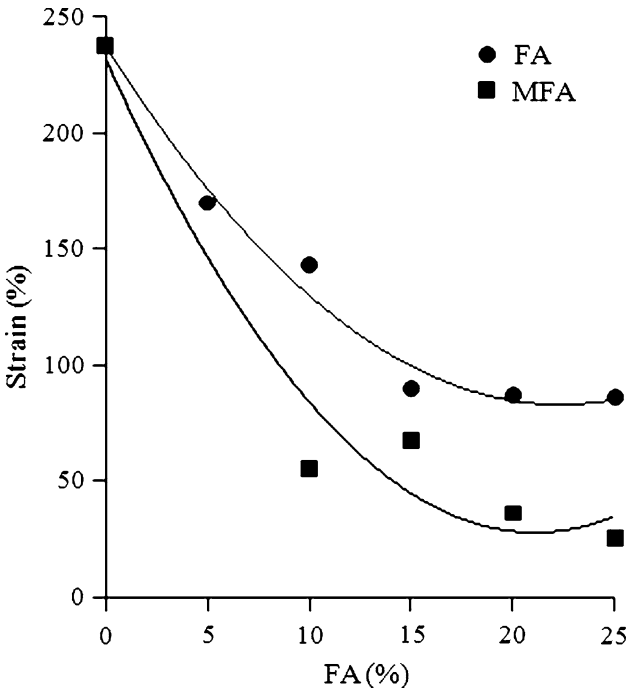

Fig. 3 The strains of the composite films with function of FA and MFA

to 289% at 20 wt% MFA than compared with FA in Fig. 2. The failure of load transfer between polymer and filler resulted in localized stress. The local stress propagated and finally translated readily into catastrophic fracture [18, 33]. The plausible explanation of higher strength of the films with MFA is the formation of stronger interfacial interaction by chemical reactions amongst PVA, MFA and GLA.

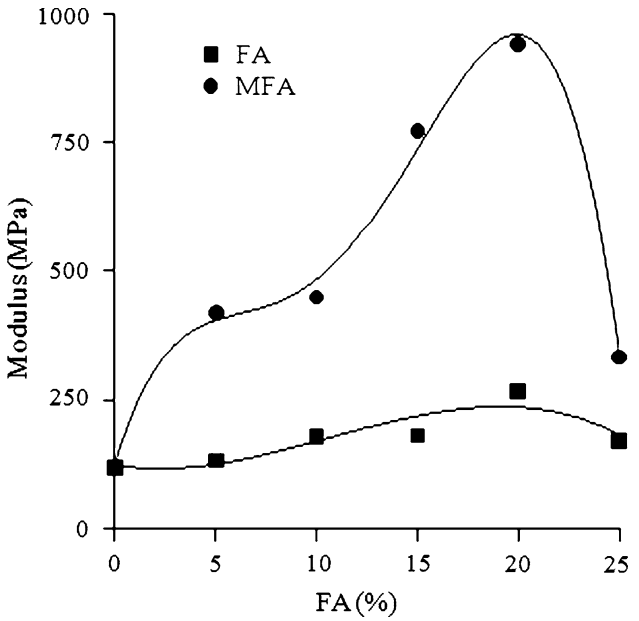

Fig. 4 The plots of Young modulus of composite films with FA and MFA

The general phenomena of the strains at failures in Fig. 3 decreased with increasing of irrespective FA/MFA additions, although some scattered values appeared in both composite films. The interfacial interactions cause restriction in the mobility of molecular chain of PVA and result in brittle behaviour [2, 21]. The moduli of the composite films are increased proportionally with FA/MFA additions. The magnitudes of strength of the films with MFA were tougher than those of the films with FA as shown in Fig. 4.

The nature and concentration of alkali is considered to play a role in formation of new crystalline phase of zeolite family. Highly concentrated 12 M NaOH solutions activated the FA particles, making them very porous, and leaving a crust of reaction product [27]. The composite films of FA modified by 4 M NaOH displayed substantial increase the levels of brittleness and harder to run the tensile test. The optimum condition for modification of high silica content of FA is 2 M NaOH.

Morphology of composite films

SEM images of tensile-fractured films were taken to study the morphological features and the representative images of 20 wt% FA/MFA composite films were displayed in Fig. 5.

The finely distributed FA/MFA particles were effectively covered by amorphous PVA chains to result in an ideal networked interface [31]. SEM images demonstrate the efficient packing of MFA in composite films along with minimal amounts of interstitial voids or porosities [33]. The interstitial voids may come from the selective

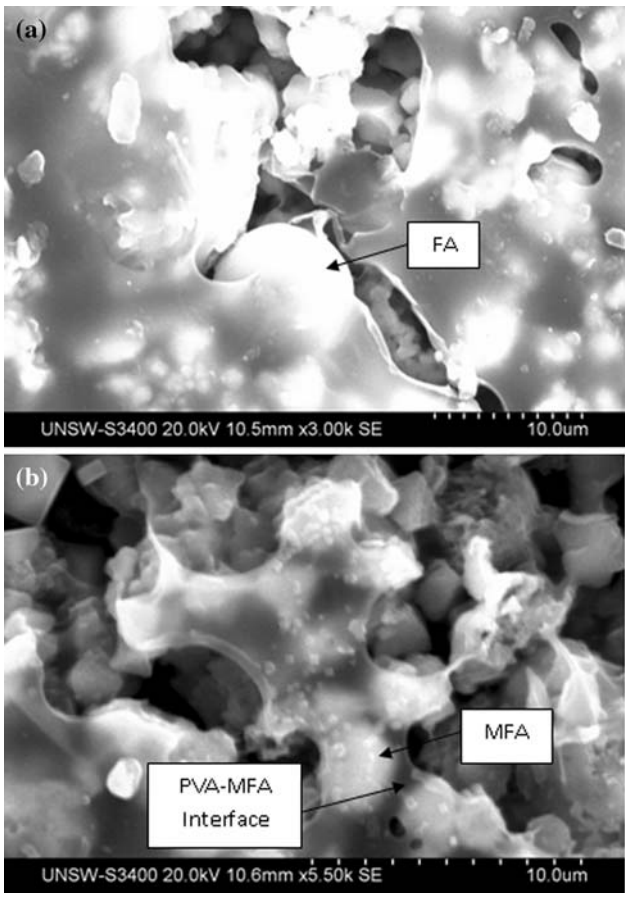

Fig. 5 SEM image of morphology of composite, **a** 20 wt% FA and **b** 20 wt% MFA films

chemical reaction of –CHO and –OH in the formation of acetal ring and ether linkage. The selective bulky acetal ring may retain a space that retards to come in intimate contact of PVA chains and MFA particles. The interface allows the stress transfer smoothly between MFA and PVA under load in mechanical test.

In the absence of maximum level interstitial voids, the composites have less ability to create local stress and the local stress mainly responsible to initiate crack. The crack then propagates and finally fracture failure happens. In terms of elongation behaviour, the inter-connectivity restricts strongly the mobility of the segmental chains of polymer and results the lower elongation rather than neat matrix [34]. The composite materials, therefore, show higher tensile strength and lower elongation, which is explained in mechanical Sect. 3.2.

Surface topography of composite films

The surface topography of the materials was defined quantitatively by mean roughness (R_a), maximum roughness (R_{max}) and root mean square (RMS) values. The

Table 2 Calculated surface roughness of the composite films

Samples	Mean roughness R_a (nm)	Maximum roughness R_{max} (μm)	Root mean square RMS (nm)
PVA + 20% FA	425.4	2.4	502.1
PVA + 20% FA + 1% GLA	471.1	3.2	610.5
PVA + 20% MFA + 1% GLA	219.3	1.9	298.0

definitions of all these terms are reported elsewhere [35]. The surface topography of modified and non-modified 20 wt% FA/MFA film materials was analysed by AFM, and the calculated results were summarized in Table 2. The values were calculated by software nanoscope III v5.12b42 installed in AFM on the images of 15 × 15 μm.

The values of R_a, R_{max} and RMS in the case of FA composite films without GLA are found to be 425.4, 2.4 and 502.1, whereas in the presence of GLA, the values are higher: 471.1 nm, 3.2 μm and 610.4, respectively. The cross-linking reaction develops roughness and porosity by 10% (R_a), 33% (R_{max}) and 22% (RMS) by forming of interstitial voids. On the other hand, the above values in the films of 20% MFA are lower: 219.3, 1.9 and 298.0, respectively. This result indicates that the existing surface increased in smoothness by 53% (R_a), 41% (R_{max}) and 51% (RMS) due to a different needle type crystalline phase of MFA in the composite. This result is consistent with the SEM and mechanical test results, which have been explained in the above-mentioned subsections, and the similar behaviour was reported in other composite systems elsewhere [35].

Characterization of composite films

The structural configurations of neat PVA and composites are characterized by FTIR spectroscopy, and the spectra are displayed in Fig. 6. The selected peaks are assigned according to references [5, 11, 12, 36, 37] and displayed in Table 3.

A broad absorption band which reflects the combination of –OH groups in PVA and adsorbed water is centred at 3298 cm^{-1} [11]. A set of absorption bands at 3298 cm^{-1} of –OH stretching, 2924 and 2875 cm^{-1} of C–H stretching, 1732 cm^{-1} of C=O stretching, 1419 and 1375 cm^{-1} of C–H/–O–H bonding, and 1090 cm^{-1} of C–O–H stretching appeared in neat PVA [34]. The peaks at 3298 cm^{-1} of –OH stretching, 2924 and 2875 cm^{-1} of C–H stretching in neat PVA molecules were significantly shifted to lower wave number along with slightly lower intensities. The shifting of intensities and wave number of the functional groups of PVA in the composites compared to neat PVA

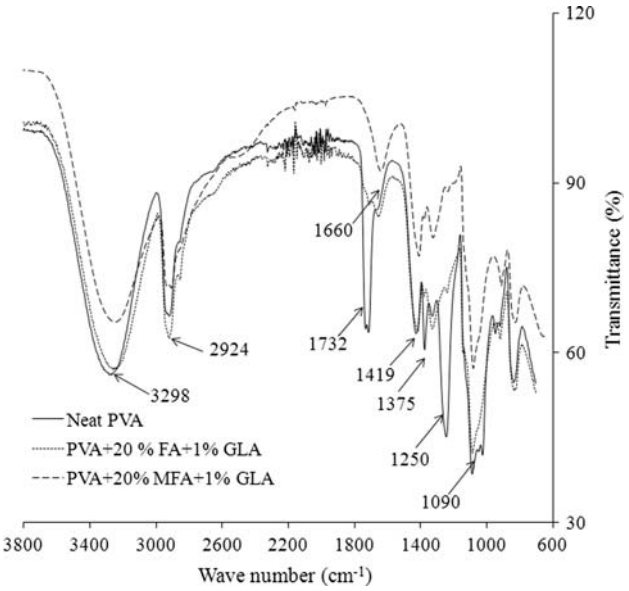

Fig. 6 FTIR spectra of neat PVA and its composite films with FA and MFA

indicated the existence of potential inter-molecular and/or intra-molecular hydrogen bonding between MFA and PVA chains [12].

The plausible hydrogen bonding mechanism of PVA and FA is recently reported [21]. The hydrogen bonding partially anchored the high modulus of MFA particles to the segments of PVA chains. The restricted mobility of PVA chain, therefore, resulted in the reduction of ductility under load and enhanced the transferring of the load between MFA and PVA chains.

The absorption bands at 1732, 1375 and 1250 cm^{-1} in PVA chains disappeared whilst the new peaks appeared at 1662 and 1385 cm^{-1}. The disappearance and re-appearance of peaks were attributed to the formation of bonds chemically in the presence of GLA. The aldehydic characteristics peak at 1720 cm^{-1} for GLA did not appear in the composite materials. This indicates the amount of cross-linking agent added to the composites mixtures, which was converted from –OH groups to the acetal ring as evidenced by the band at 1385 cm^{-1} [8].

The appearance of absorption peak at 1385 cm^{-1} reflects the possible pathways of chemical reactions in terms of ternary components, PVA, MFA and GLA in the formation of acetal ring and ether linkage, and the mechanistic scheme for reaction mechanism is shown in Fig. 7 considering all the phenomena discussed above. All of the possible chemical reactions allowed the formation of a new covalent Si–O–C bridge on the surface of MFA particles and the interfacial bond tenaciously anchoring the PVA chains. The mobility of PVA chains is thus severely restricted under load in the mechanical test [32].

Table 3 Selected FTIR absorption peaks in neat PVA and composite films

Samples	Peak positions of structural groups (cm^{-1})						
	OH str	C–H str/bend	C=O str	O–H bend	C–H bend	C–O–C str	C–OH str
PVA	3298	2924/2875	1732	1419	1375	1250	1090
PVA + 20% FA + 1% GLA	3271	2900/2879	1662	1412	1383	1244	1090
PVA + 20% MFA + 1% GLA	3271	2943	1660	1423	1336	1263	1090

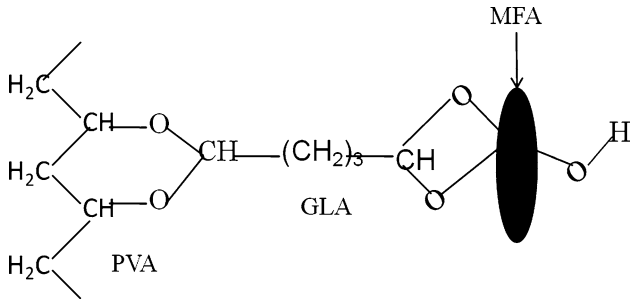

Fig. 7 A plausible diagram of chemical bonding in the ternary systems, PVA, MFA and GLA

Conclusions

In conclusion, the key points of this study are highlighted as follows:

The alkali-activated spherical MFA particles were finely distributed in PVA matrix. This led to a proportional increase in the tensile strength. The maximum strength was found with the addition of 20 wt% MFA. Further addition beyond this amount resulted in a downward trend because of super saturation of particles in composite system. The modification of FA led to a 289% increase in strength compared to the control, and induced a strength 414% higher than neat PVA film under an identical condition.

The decrease in strength with higher amounts of MFA addition is due to the reduction of intimate contact between the surfaces of MFA and PVA chains. The intimate contact may come from the hydrogen and chemical bonding between the two surfaces which then form a type of network. This efficiently transfers load without creating localized stress.

In the examination of the morphology and topography of the composite materials, the inter-connecting bridges in the composite films were observed by SEM. This was irrespective of FA additions. A minimum level of porosity and interstitial voids was also visualized. The modification of FA resulted in a smoother film surface. According to AFM calculation, needle-type zeolite crystal in MFA makes film surface smoother by 53% (R_a), 41% (R_{max}) and 51% (RMS) compared with unmodified spherical FA composite films.

References

1. Ray SS, Okamoto M (2003) Prog Polym Sci 28:1539
2. Tjong SC, Li RKY, Cheung T (1997) Polym Eng Sci 37(1):166
3. Bigg DM (1987) Polym Comp 8(2):115
4. Chiellini E, Cinelli P, Imam SH, Mao I (2001) Biomacromolecules 2:1029
5. Ramaraj B (2007) J Appl Polym Sci 103:909
6. Strawhecker KE, Manias E (2000) Chem Mater 12:2943
7. Zhang X, Liu T, Sreekumar TV, Kumar S, Moore VC, Hauge RH, Smalley R (2003) Nano Lett 3(9):1285
8. Bana R, Banthia AK (2007) Polym-Plast Tech Eng 46:821
9. Weichold O, Moller M (2007) Adv Mater 9(8):712
10. Tan LS, Mchugh AJJ (1996) Mater Sci 31:3701
11. Chen X (2002) J Mater Sci Lett 21:1637
12. Huang H, Gu L, Ozaki Y (2006) Polymer 47:3935
13. Ward CR, French D (2006) Fuel 85:2268
14. Alkan C, Arslan M, Cici M, Kaya M, Aksoy M (1995) Resour Conver Recyl 13:147
15. Kojima Y, Usuki A, Kawasumi M, Fukushima Y, Okada A, Kurauchi T, Kamigaito O (1993) J Mater Res 8:1179
16. Guhanathan S, Sarojadevi M (2004) Comp Interface 11(1):43
17. Gupta N, Brar BS, Woldesenbet E (2001) Bull Mater Sci 24(2):219
18. Nath DCD, Bandyopadhyay S, Yu A, Zeng Q, Das T, Blackburn D, White C (2009) J Mater Sci 44:6078. doi:10.1007/s10853-009-3839-3
19. Nath DCD, Bandyopadhyay S, Yu A, Blackburn D, White C (2010) J Appl Poly Sci 115:1510
20. Nath DCD, Bandyopadhyay S, Yu A, Blackburn D, White C, Varughese S (2009) J Therm Anal Calorim. doi:10.1007/s10973-009-0408-6
21. Nath DCD, Bandyopadhyay S, Boughton P, Yu A, Blackburn D, White C (2009) J Appl Poly Sci. doi:10.1002/app.31635
22. Nath DCD, Bandyopadhyay S, Yu A, Blackburn D, White C (2010) J Mater Sci 45:1354. doi:10.1007/s10853-009-4091-6
23. Nath DCD, Bandyopadhyay S, Gupta S, Yu A, Blackburn D, White C (2009) Appl Surf Sci. doi:10.1016/j.apsusc.2009.11.024
24. Fan Y, Yin S, Wen Z, Zhong J (1999) Cem Concr Res 29:467
25. Jimenez AF, Palomo A (2003) Fuel 82:2259
26. Brouwers HJH, Eijk RJV (2003) Proceedings of the 11th international congress on the chemistry of cement (ICCC). In: Cements contribution to the development in the 21st century, ISBN No: 0-9584085-8-0. Durban, South Africa, 11–16 May 2003
27. Palomo A, Grutzeck MW, Blanco MT (1999) Cem Concr Res 29:1323
28. Tanaka H, Furusawa S, Hino R (2002) J Mater Syn Process 10(3):143
29. Palomo A, Blanco MT, Granizo ML, Puertas F, Vazquez T, Grutzeck MW (1999) Cem Concr Res 29:997
30. Chang HL, Shih WH (1998) Ind Eng Chem Res 37:71
31. Jimenez AF, Palomo A (2005) Cem Concr Res 35:1984

32. Immelman E, Sanderson RD, Jacobs EP, Reenen AJV (1993) J Appl Polym Sci 50:1013
33. Tan LS, Mchugh AJ (1996) J Mater Sci 31:3701. doi:10.1007/BF00352783
34. Leong YW, Bakar MBA, Ishak ZAM, Ariffin A, Pukanszky B (2004) J Appl Polym Sci 91:3315
35. Arfat A, Banthia AK, Bandyopadhyay S (2008) J Power Sour 179:69
36. Yurudu C, Isci S, Unlu C, Atici O, Ece I, Gungor N (2006) J Appl Polym Sci 102:2315
37. Kaczmarek H, Podgorski A (2007) J Photochem Photobio A Chem 191:209